Psychological Medicine

cambridge.org/psm

Resolving heterogeneity in depression using individualized structural covariance network analysis

Shaoqiang Han[1,2,3,4,5,6,7,8], Ruiping Zheng[1,2,3,4,5,6,7,8], Shuying Li[9], Bingqian Zhou[1,2,3,4,5,6,7,8], Yu Jiang[1,2,3,4,5,6,7,8], Keke Fang[10], Yarui Wei[1,2,3,4,5,6,7,8], Jianyue Pang[9], Hengfen Li[9], Yong Zhang[1,2,3,4,5,6,7,8], Yuan Chen[1,2,3,4,5,6,7,8] and Jingliang Cheng[1,2,3,4,5,6,7,8]

[1]Department of Magnetic Resonance Imaging, the First Affiliated Hospital of Zhengzhou University, Zhengzhou, China; [2]Key Laboratory for Functional Magnetic Resonance Imaging and Molecular Imaging of Henan Province, Zhengzhou, China; [3]Engineering Technology Research Center for Detection and Application of Brain Function of Henan Province, Zhengzhou, China; [4]Engineering Research Center of Medical Imaging Intelligent Diagnosis and Treatment of Henan Province, Zhengzhou, China; [5]Key Laboratory of Magnetic Resonance and Brain Function of Henan Province, Zhengzhou, China; [6]Key Laboratory of Brain Function and Cognitive Magnetic Resonance Imaging of Zhengzhou, Zhengzhou, China; [7]Key Laboratory of Imaging Intelligence Research Medicine of Henan Province, Zhengzhou, China; [8]Henan Engineering Research Center of Brain Function Development and Application, Zhengzhou, China; [9]Department of Psychiatry, the First Affiliated Hospital of Zhengzhou University, Zhengzhou, China and [10]Department of Pharmacy, Affiliated Cancer Hospital of Zhengzhou University, Henan Cancer Hospital, Zhengzhou, China

Abstract

Background. Elucidating individual aberrance is a critical first step toward precision medicine for heterogeneous disorders such as depression. The neuropathology of depression is related to abnormal inter-regional structural covariance indicating a brain maturational disruption. However, most studies focus on group-level structural covariance aberrance and ignore the interindividual heterogeneity. For that reason, we aimed to identify individualized structural covariance aberrance with the help of individualized differential structural covariance network (IDSCN) analysis.

Methods. T1-weighted anatomical images of 195 first-episode untreated patients with depression and matched healthy controls ($n = 78$) were acquired. We obtained IDSCN for each patient and identified subtypes of depression based on shared differential edges.

Results. As a result, patients with depression demonstrated tremendous heterogeneity in the distribution of differential structural covariance edges. Despite this heterogeneity, altered edges within subcortical-cerebellum network were often shared by most of the patients. Two robust neuroanatomical subtypes were identified. Specifically, patients in subtype 1 often shared decreased motor network-related edges. Patients in subtype 2 often shared decreased subcortical-cerebellum network-related edges. Functional annotation further revealed that differential edges in subtype 2 were mainly implicated in reward/motivation-related functional terms.

Conclusions. In conclusion, we investigated individualized differential structural covariance and identified that decreased edges within subcortical-cerebellum network are often shared by patients with depression. The identified two subtypes provide new insights into taxonomy and facilitate potential clues to precision diagnosis and treatment of depression.

Introduction

As a heterogeneous disorder, depression is characterized by diverse symptom profiles and treatment responses (Kessler et al., 2003; Yu et al., 2019). The diversity of symptoms is suggested to originate from imbalanced coordination among large-scale brain networks (Kaiser, Andrews-Hanna, Wager, & Pizzagalli, 2015). Recently, progress in neuroimaging research studies provides powerful tools to probe network-level interactions. Among them, structural covariance describes the coordinated regional volumes between brain regions reflecting their common development/maturation trajectories (Alexander-Bloch, Giedd, & Bullmore, 2013; Yun, Jang, Kim, Jung, & Kwon, 2015). Structural covariance among brain regions is hypothesized to be related to anatomical connectivity (Lerch et al., 2006) and can be influenced by mutual brain-derived neurotrophic factor (Pezawas et al., 2004) and activity-dependent structural plasticity (Draganski et al., 2004). Compared with widely used functional connectivity, structural covariance measures brain connectivity features on a larger time scale representing maturational/trait-like connection features (Evans, 2013). Structural covariance is implicated in

Original Article

Cite this article: Han S *et al* (2023). Resolving heterogeneity in depression using individualized structural covariance network analysis. *Psychological Medicine* **53**, 5312–5321. https://doi.org/10.1017/S0033291722002380

Received: 16 February 2022
Revised: 5 June 2022
Accepted: 12 July 2022
First published online: 12 August 2022

Key words:
Depression; gray matter volume; heterogeneity; individualized analysis; subtypes of depression

Authors for correspondence:
Shaoqiang Han,
E-mail: shaoqianghan@163.com;
Yuan Chen,
E-mail: chenyuanshizt@163.com;
Jingliang Cheng,
E-mail: fccchengjl@zzu.edu.cn

© The Author(s), 2022. Published by Cambridge University Press

cognitive/behavioral abilities and can be reshaped by normal development, aging and mental disease (Alexander-Bloch et al., 2013).

The neuropathology of depression is related to abnormal neurodevelopment trajectories in distributed brain regions and interregional connections (Kaiser et al., 2015; Lima-Ojeda, Rupprecht, & Baghai, 2018). However, diversity of symptom profiles, etiologies, treatment responses and neuroimaging phenotypes consistently argue that depression is a highly heterogeneous disorder possibly without a unifying neuropathology (Bondar, Caye, Chekroud, & Kieling, 2020; Drysdale, Grosenick, & Downar, 2017; Krishnan & Nestler, 2008). Traditional case-control designs often focus on group-level aberrance while ignore the interindividual heterogeneity (Wolfers et al., 2018). Although studies have revealed altered structural covariance in depression, most of them exclusively probe group-level aberrance (Mak, Colloby, Thomas, & O'Brien, 2016; Rashidi-Ranjbar et al., 2020; Yun & Kim, 2021). Depicting individualized structural differences helps us to discover neuroimaging substrates underlying symptoms and uncover more homogeneous subtypes in heterogeneous disorders (Ajnakina et al., 2021; Das et al., 2018).

A growing number of researchers begin to acknowledge the high interindividual heterogeneity and investigate individualized neuroimaging differences in mental disorders such as schizophrenia (Voineskos, Jacobs, & Ameis, 2020). Sun et al. identify that high interindividual heterogeneity leads to inconsistent neuroimaging findings in schizophrenia (Sun et al., 2021). Wolfers et al. using normative model parsing heterogeneity under clinical conditions find that bipolar disorder and schizophrenia are highly heterogeneous and group-level differences disguise biological the heterogeneity (Wolfers et al., 2018). Lv et al. adopt quantile regression to deduce normative ranges of subject-level brain structure from age and sex. They find that group-level structural difference introduced by schizophrenia is not on behalf of most patients (Lv, Di Biase, Cash, & Cocchi, 2020). Especially, Liu et al. propose individualized differential structural covariance network (IDSCN) analysis method making it possible that inferring individualized differential structural covariance. Using this method, they discover two neuroanatomical subtypes of schizophrenia with distinct symptom profiles, resolving the clinical and biological heterogeneity in schizophrenia (Liu et al., 2021).

In this study, we aimed to describe subject-level differential structural covariance aberrance in depression by employing IDSCN analysis method. This study was organized as follows. First, we investigated the degree of morphological heterogeneity in depression. Considering the multifarious symptoms and treatment responses, we expected to find higher morphological heterogeneity in patients with depression than that in healthy controls (HCs). Second, we obtained individualized differential structural covariance edges for each patient with depression. Third, we clustered patients with depression into subtypes where shared individualized differential structural covariance edges were treated as features and examined neuroimaging and clinical phenotypes of each subtype.

Materials and methods

Sample

The study was approved by the research ethical committee of the First Affiliated Hospital of Zhengzhou University. For each participant, written informed consent was obtained before experiment. We recruited first-episode untreated patients with depression ($n = 195$) from out-patient services of the Department of Psychiatry, the First Affiliated Hospital of Zhengzhou University, Zhengzhou, China. The diagnosis was done by one chief physician and one well-trained psychiatrist according to Diagnostic and Statistical Manual of Mental Disorders, Fourth Edition (DSM-IV) for depression. Patients would be excluded if they met one of the exclusion criteria: (1) comorbidity with other mental (psychotic) disorders and (2) a history of manic symptoms. All patients were during depressed phase. The clinical states were evaluated using the 17-items Hamilton Depression scale (HAMD). Matched HCs ($n = 78$) were recruited from the community through poster advertisement. All HCs were Han Chinese and right handedness. None of them had a history of serious medical, neuropsychiatric illness, family history of major psychiatric or neurological illness in their first-degree relatives.

In addition, all participants must meet the following exclusion criteria: (1) taking drugs such as anesthesia, sleeping and analgesia in the past 1 month; (2) substance abuse; (3) a history of brain tumor, trauma, surgery or other organic body disease; (4) suffering from cardiovascular diseases, diabetes or hypertension; (5) contraindications for magnetic resonance imaging (MRI) scanning and (6) other structural brain abnormalities revealed by MRI scan.

Data acquisition

T1-weighted anatomical images of participants in dataset 1 were acquired using on 3-Tesla GE Discovery MR750 scanner (General Electric, Fairfield Connecticut, USA). Using an eight-channel prototype quadrature birdcage head coil, we acquired structural T1-weighted images with 3D-spoiled gradient echo scan sequence with the following parameters: repetition time = 8164 ms, echo time = 3.18 ms, inversion time = 900 ms, flip angle = 7 degrees, resolution matrix = 256 × 256, slices = 188, thickness = 1.0 mm, voxel size = 1 × 1 × 1 mm^3.

Voxel-based morphometry analysis

All scans were processed following the standard pipeline of CAT12 toolbox (http://dbm.neuro.uni-jena.de/cat12/). Main steps included: bias-field correction, segmentation (gray and white matter and cerebrospinal fluid), adjustment for partial volume effects, normalization into Montreal Neurological Institute space, resampled to 1.5 mm × 1.5 mm × 1.5 mm and nonlinear modulation. Finally, the gray matter maps were smoothed using 6 mm full width at half maximum Gaussian kernel. The total intracranial volume (TIV) of each participant was also calculated for the following analysis.

Morphological heterogeneity and group difference

We explored whether patients with depression exhibited higher morphological heterogeneity than HCs adopting the following steps: (1) constructing a group-level $M \times M$ (M, the number of brain regions in brain atlas) structural covariance network (SCN) for each group. The 268 brain atlas was chosen for the reason that functional connectome built based on it turned out a 'fingerprint' (Finn et al., 2015; Shen, Tokoglu, Papademetris, & Constable, 2013). (2) A jackknife-bias estimation procedure was used to determine individual's contribution to the overall group-level SCN, thus deriving individualized SCN for each subject (Das et al., 2018; Miller & Rupert, 1974). (3) The Euclidean distance value was calculated to measure the deviation between subject-level and group-level SCNs for each subject. The average

https://doi.org/10.1017/S0033291722002380 Published online by Cambridge University Press

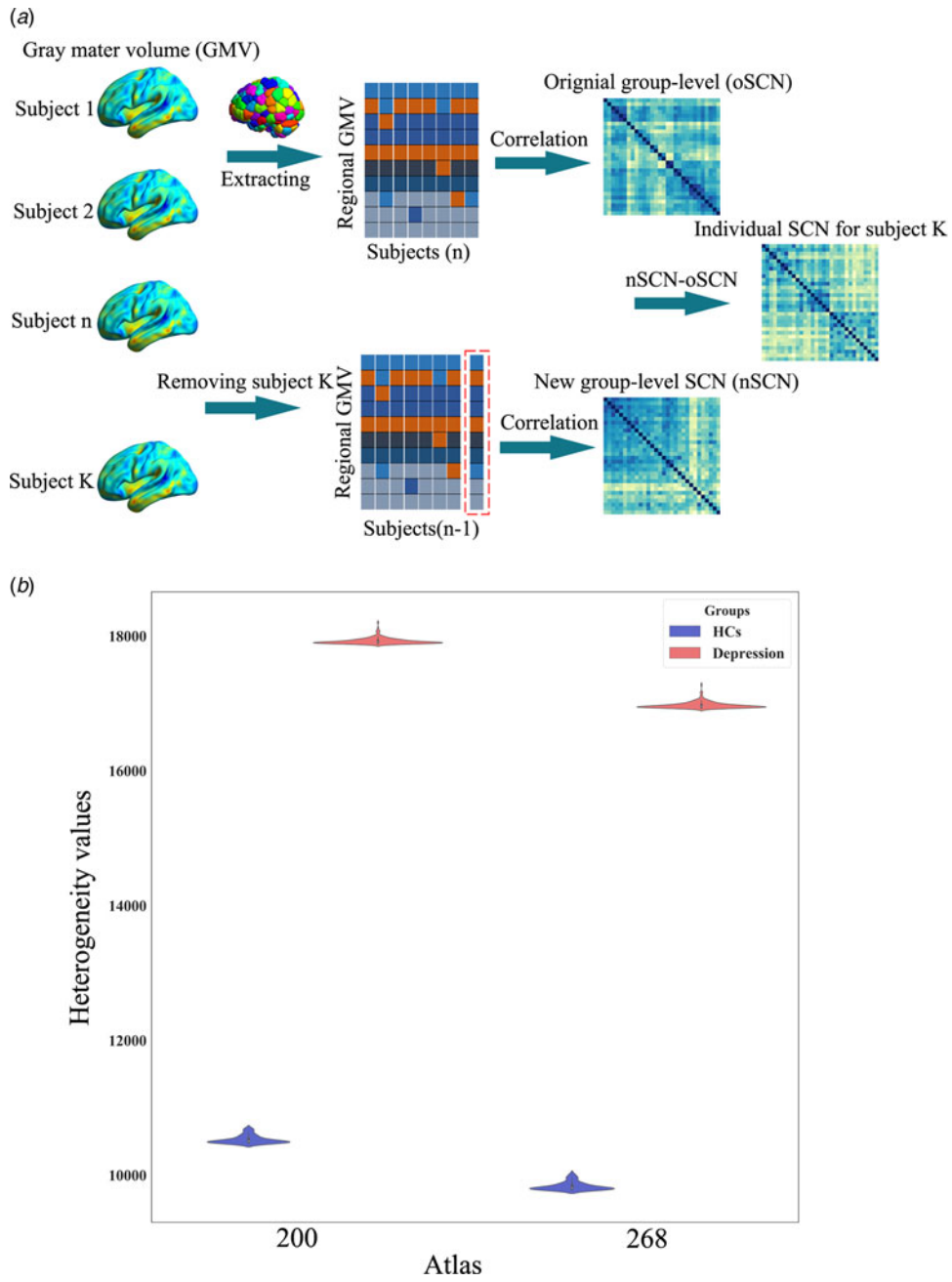


Fig. 1. Workflow for calculating individualized SCN. (a) Procedure of calculating individualized SCN. First, we obtained original group-level SCN (oSCN) and new group-level SCN (nSCN) by removing subject *k* from original group. Then, the individual SCN for subject *k* was defined as: nSCN − oSCN. This procedure was done in patients and HCs separately. (b) We calculated Euclidean distance between individualized SCN and group-level SCN for each subject. The heterogeneity (variability) values were compared between patients with depression and HCs using two-sample *t* test.

distance (heterogeneity) value determined the degree of morphological heterogeneity for one group (Fig. 1a). Heterogeneity values were compared between patients with depression and HCs using Wilcoxon rank sum test controlling for age, sex, education level and TIV. We also validated this result with another brain atlas (200 regions) (Craddock, James, Holtzheimer, Hu, & Mayberg, 2012).

Constructing the IDSCN

To measure the individualized differential structural covariance, we adopted a newly proposed method named IDSCN analysis (Liu et al., 2021). Here, we just briefly described the main steps; more details could be seen in Liu et al. (2021). (1) Constructing the reference structural covariance network (rSCN) using all HCs by calculating partial correlation between regional gray matter volume (GMV) for each pair of brain regions where age, gender and educational level and TIV were treated as covariates. (2) Adding one patient *k* into HCs as a new group. A perturbed structural covariance network (pSCN) was built with the new group. (3) The difference (ΔSCN) between the pSCN and rSCN was calculated: ΔSCN = pSCN − rSCN. (4) Calculating the *Z*-score of ΔSCN according to the following formula:

https://doi.org/10.1017/S0033291722002380 Published online by Cambridge University Press

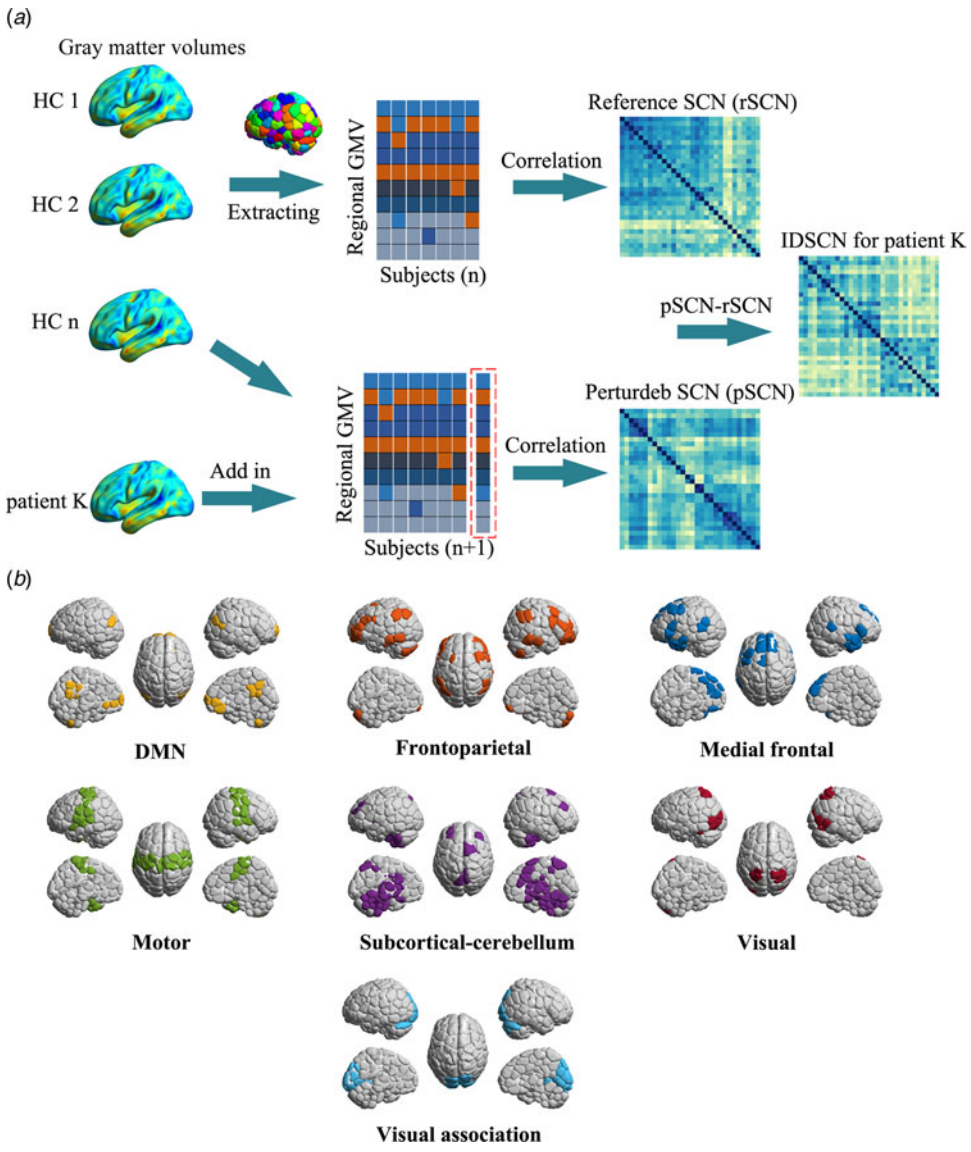


Fig. 2. Workflow of IDSCN and network definition in this study: (a) description of obtaining IDSCN for patient *k* and (b) nodes and networks in 268 brain atlas.

$$Z = \frac{\Delta \mathrm{SCN}}{(1 - \mathrm{rSCN}^2)/(n-1)}$$

The IDSCN for patient *k* was constructed with the *Z*-scores obtained from the *Z* test. Positive *Z*-scores represented higher structural covariance edges strength in patient *k* against the reference HCs or vice versa. The *p* values of edges were obtained from the *Z*-scores. Then, we identified individualized differential structural covariance edges that were significantly different from the reference SCN in each patient with $p < 0.05$, Bonferroni corrected for $268 \times 267/2 = 35\,778$ edges (Fig. 2).

Subtyping patients with depression

Then, we clustered patients with depression by adopting the *k*-means method where the top 100 differential structural covariance edges as features. The optimal cluster number ranging from 2 to 10 was determined by silhouette values (Liu et al., 2021). We did not choose the top edges shared by 5% of patients as done in Liu et al. (2021) for the reason that there was only one edge shared more than 10 patients (5% of 195 patients). The *k*-means was repeated 100 times to avoid local minima resulted from random in initialization of centroid positions (Allen et al., 2014).

Reproducibility analysis

To further inquire the reproducibility of subtyping results, we adopted different strategies. (1) Using another brain atlas (200 regions). (2) Using different numbers of top differential edges (80 or 120). The adjusted Rand index (ARI) was used to quantify the consistency of subtyping results between these subtyping results (Hu Be Rt & Arabie, 1985). (3) To exclude the change that subtyping results were driven by a few subjects, we randomly selected 80% of patients and performed the same subtyping results on the sub-samples. ARI value was calculated between the subtyping results obtained from sub-samples and that from the whole dataset (all patients). This procedure was repeated 100 times.

https://doi.org/10.1017/S0033291722002380 Published online by Cambridge University Press

Table 1. Demographic and clinical characteristics of participants

	HC ($N = 78$)	Depression ($N = 195$)	p
Male, no. (%)	40 (51.28)	95 (48.7)	0.95[a]
Age, mean (s.d.) [range], years	17.85 (4.29) [12–34]	18.14 (4.47) [11–37]	0.62[b]
Educational level, mean (s.d.), years	10.51 (2.80)	10.11 (2.13)	0.22[b]
Duration of illness, mean (s.d.), months	–	15.74 (16.96)	
HAMD score, mean (s.d.), [range]	–	22.38 (5.72) [12–48]	
Handedness, right/left	130/0	195/0	
Age of first onset, years	–	16.81 (4.40)	

HAMD, Hamilton Rating Scale for Depression; HC, healthy control.
[a]χ^2 t test.
[b]Two-tailed two-sample t test.

Clinical and IDSCN examination of depression subtypes

Then, we examined differences between subtypes of depression in terms of age, sex, education level, TIV, duration of illness and the total score of HAMD with two sample t test or chi-square test accordingly. The top 100 differential edges were organized into between- and within-network edges defined in the previous study (Finn et al., 2015) and then compared between subtypes of depression using two sample t test.

Functional annotation of altered structural covariance edges

Integrating results of a great number of neuroimaging studies, Yarkoni et al. provided probabilistic (activation) mappings supporting quantitative inferences about association between cognitive process with regional brain activity (Neurosynth, https://neurosynth.org/) (Yarkoni, Poldrack, Nichols, Van Essen, & Wager, 2011). Each voxel in one activation map was associated with the numbers of terms/tasks helping to interpret the function of that region (Yarkoni et al., 2011). There were more than 3000 search terms with their activation maps provided by Neurosynth. Among these, 217 terms bore clear biological significance (details of the selection criteria were described in Cheng et al., 2017). To provide a further interpretation for identified differential structural covariance edges in each subtype, functional annotation analysis was performed to investigate association between altered structural covariance edges and cognitive states using activation maps provided by Neurosynth (Han et al., 2022). Differential structural covariance edges were determined where $p < 0.005$ (uncorrected) for each subtype compared with HCs. The tolerant p value was determined to include the potential altered edges in each subtype in consideration of high level of heterogeneity in depression (see below). Altered edges were associated with functional terms using the mean co-activation ratio measuring the extent of edges for a functional term, the significance were determined using permutation test (Liu et al., 2019). This procedure was done using brain annotation toolbox (BAT, http://123.56.224.61/softwares) (Liu et al., 2019).

Results

Clinical demographics

The clinical and demographic information is included in Table 1. As we could see, patients with depression presented no difference with HCs in terms of age, sex and educational level.

Higher morphological heterogeneity in patients with depression

Patients with depression exhibited higher heterogeneity values than HCs ($Z = 12.90$, $p < 0.001$, Cohen's $d = 140.512$). This result was validated with 200 brain atlas ($Z = 12.91$, $p < 0.001$, Cohen's $d = 137.999$) (Fig. 1b). These results suggested high structural interindividual heterogeneity in patients and the necessity of investigating individualized structural aberrance in depression.

Heterogeneity of IDSCN in depression

For each patient with depression, we obtained differential structural covariance edges ($p < 0.05$, Bonferroni corrected for 35 778 edges). Patients with depression demonstrated highly heterogeneous differential edges from patient to patient. Specially, among all edges, 28 462 differential edges were shared by at least one patient and 9102 differential edges were shared by at least two patients. The distribution of shared differential edges is included in online Supplementary Fig. S1.

To map the distribution of differential edges across patients, we organized the top 100 differential edges into within- and between-network edges. The networks were defined according to the previous study (Finn et al., 2015) where 268 regions were divided into seven networks (Fig. 2b). The numbers of edges between- and within-network are shown in Fig. 3a. As we could see, these edges were mainly distributed within subcortical-cerebellum network, between subcortical-cerebellum network and motor network.

Two distinct neuroanatomical subtypes of depression identified by IDSCN

We clustered patients with depression using the top 100 differential edges obtained from all patients. Two subtypes were identified (subtype 1, $N = 105$; subtype 2, $N = 90$). The silhouette values are shown in online Supplementary Fig. S2. Among the top 100 edges, these two subtypes exhibited significant differential edges within subcortical subcortical-cerebellum network, between medial frontal network and motor edges and between subcortical-cerebellum network and visual network. The details are included in online Supplementary Fig. S3, where the significant differential edges are marked with '*'. The differential between- and within-network edges of each subtype compared with HCs were also

https://doi.org/10.1017/S0033291722002380 Published online by Cambridge University Press

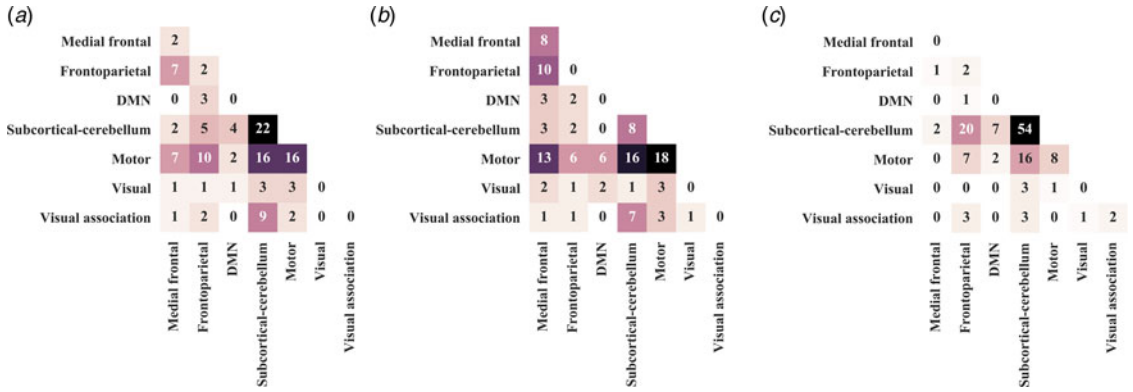


Fig. 3. Distribution of individualized differential edges and subtyping results. (a) The overlapping differential edges in IDSCN in all patients. As we could see, these edges were mainly distributed within subcortical-cerebellum network. (b) The distribution of shared differential edges in subtype 1. (c) The distribution of shared differential edges in subtype 2.

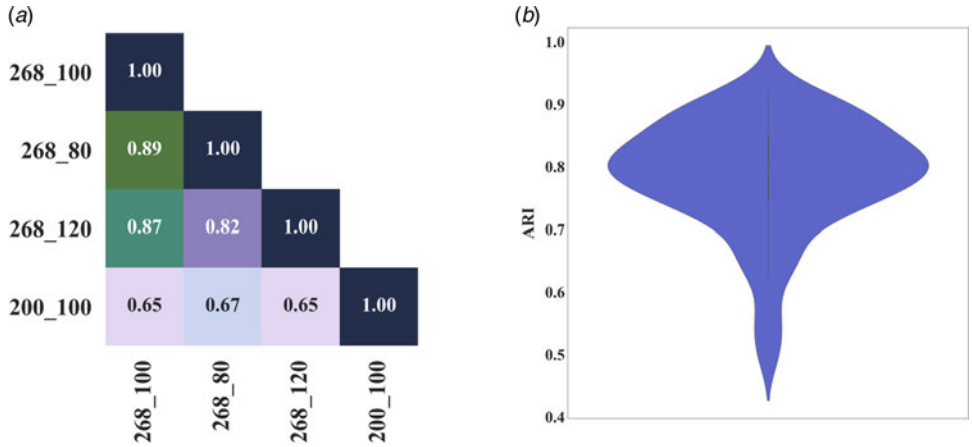


Fig. 4. Reproducibility of subtyping results. (a) ARI values between results based on different brain atlases and numbers of top differential edges. E.g. '268_100' represented subtyping results based on the top 100 differential edges with 268 brain regions atlas. (b) Distribution of ARI values between subtyping results randomly selected sub-samples and that of all patients.

obtained (online Supplementary Fig. S3). These two subtypes exhibited decreased edges compared with HCs.

For each subtype, we also obtained the top 100 differential edge whose distribution is shown in Figs 3b and 3c. As we could see, most patients of subtype 1 shared decreased edges within motor network and its connections with other networks including medial frontal network and subcortical-cerebellum network. Patients of subtype 2 shared decreased edges within subcortical-cerebellum network and its connections with frontoparietal and motor network.

Although demonstrating remarkable neuroanatomical aberrance these two subtypes shared indistinguishable clinical and demographic features including duration of illness, the total score of HAMD, age, sex and TIV (all p values > 0.05).

Subtyping results present robust reproducibility

Subtyping results showed robust reproducibility with different brain atlases and numbers of top edges. The number of subtypes was consistently two when we used another brain atlas (200 brain regions) or chose different number of top edges (80 or 120). ARI values between subtyping results are shown in Fig. 4a. ARI values between the subtyping results obtained from sub-samples and that from all patients were 0.787 ± 0.090 (Fig. 4b).

Functional annotation for differential edges in each subtype

With the help of BAT, we performed functional annotation analysis on the differential edges in each subtype of depression to associate differential edges with cognitive states. As a result, differential edges in subtype 1 were not related to any functional terms. While differential edges in subtype 2 were significantly related to functional terms ($p < 0.05$ for permutation test) such as monetary reward, motivation and reward anticipation (online Supplementary Table S1).

Discussion

For the first time, we described the individualized altered structural covariance in patients with depression. Patients with depression exhibited higher heterogeneity values than HCs suggesting high morphological heterogeneity and emphasizing the necessity of obtaining subject-level altered structural covariance in depression. Then, we identified individualized differential structural

https://doi.org/10.1017/S0033291722002380 Published online by Cambridge University Press

covariance for each patient. Patients with depression exhibited remarkable differences in distribution of differential structural covariance edges. Despite this heterogeneity, altered edges within subcortical-cerebellum network were often shared by most of the patients. Two robust subtypes were uncovered based on shared differential edges. The two subtypes exhibited distinct distributions of differential edges. Specifically, subtype 1 was characterized by decreased motor network-related edges and subtype 2 was characterized by decreased subcortical-cerebellum network-related edges. In addition, decreased edges in subtype 2 were mainly implicated in reward/motivation-related functional terms. These results hinted the subtype 1 was related to psychomotor retardation while subtype 2 was related to anhedonia.

The heterogeneity hampered the research into the mechanism of depression. Although being diagnosed as the same disorder, patients with depression exhibited diverse symptom profiles, course trajectories and treatment responses that driven by varying neurophysiological and genetic mechanisms (Lynch, Gunning, & Liston, 2020). The heterogeneity hampered the revelation of neuropathological mechanism and discovery of stabilized biomarkers to guide clinical diagnosis and treatment (Sun et al., 2021). In schizophrenia, researchers had systematically elucidated the effect of interindividual heterogeneity on observed functional connectomes (Chen et al., 2018; Cole, Anticevic, Repovs, & Barch, 2011; Gopal et al., 2016; Sun et al., 2021). They found that patients with schizophrenia exhibited higher interindividual heterogeneity in distributed brain regions than normal people and that group-level aberrance was not representative of most patients (Lv et al., 2020; Sun et al., 2021). However, the heterogeneity of depression remained unclear. Knowing this was the first step to precision diagnose and determination of follow-up treatment plan. Patients with depression exhibited higher heterogeneity values than HCs and low overlap of differential structural covariance edges with each other, suggesting higher morphological heterogeneity and emphasizing the necessity of adopting individualized analysis method in neuroimaging study of depression.

Depression was characterized by abnormal communications among large-scale brain networks encompassing distributed brain regions (Kaiser et al., 2015). Nonetheless, the findings were not consistent (Gong & He, 2015; Kaiser et al., 2015) that was usually attributed to factors such as small samples, comorbidities, medication, age of onset and sex (Han et al., 2021a, 2021b; Schmaal et al., 2017; Zhao et al., 2014). The current study demonstrated that remarkable heterogeneity still exhibited even we controlled factors including medication and comorbidities. Combing with results that identified two subtypes shared indistinguishable duration of illness, sex, age and the total HAMD score, our results revealed that high morphological heterogeneity might be inherent to the pathophysiology of depression. Although abnormal structural covariance had been reported in previous studies, they exclusively obtained group-level differential structural covariance aberrance ignoring interindividual heterogeneity (Lee et al., 2019; Neufeld & Kaczkurkin, 2020; Watanabe et al., 2020; Yun & Kim, 2021). To our knowledge, the current study was the first attempt to investigate subject-level differential structural covariance edges in depression. Although subject-level structural covariance aberrance presented notable variability across patients, shared decreased structural covariance edges within subcortical-cerebellum network were shared most patients. The subcortical-cerebellum network defined in this study encompassed regions such as hippocampus, amygdala, striatum, thalamus, orbitofrontal gyrus, anterior insula and cerebellum (Finn et al., 2015). These regions and connections among them were frequently reported and implicated in the pathophysiology of depression (Gong & He, 2015; Kaiser et al., 2015; Otte et al., 2016). Our results suggested that although presenting high heterogeneity in structural covariance aberrance, patients with depression shared decreased structural covariance connections within subcortical-cerebellum network.

To handle the heterogeneity, psychiatrists exclusively divided patients with depression into categories according to clinical manifestations (Harald & Gordon, 2012; Lynch et al., 2020). However, variations in symptom profiles explained a fraction of heterogeneity in etiology and treatment response. Similar clinical symptoms could be introduced by distinct underlying mechanisms (Goldberg, 2011; Hasler, 2010; Kendell & Jablensky, 2003). The categorical approach based on symptomatology presented too vague diagnostic threshold to handle sub-threshold symptoms and low sensitivity (Okada et al., 2015). As a consequent, subtypes based on symptomatology are found to share overlapped neuroimaging aberrance (Ravindran et al., 2020; Xia et al., 2020; Yoo et al., 2008). In recent years, researchers began to identify more homogeneous patient subtypes using data-driven methods based on neuroimaging features (Beijers, Wardenaar, van Loo, & Schoevers, 2019). To our knowledge, five studies revealed subtypes of depression with four studies using functional connectivity and one study using fractional anisotropy (Cheng et al., 2014; Drysdale et al., 2017; Feder et al., 2017; Price et al., 2017b; Price, Gates, Kraynak, Thase, & Siegle, 2017a). Compared with these studies, there were two advantages in this study. First, compared with studies using functional connectivity, we adopted structural covariance, representing more stable maturational/trait-like connection features (Evans, 2013). Second, previous studies used brain neuroimaging features while we clustered patients based on their individualized differential structural covariance edges from HCs reflecting individualized pathological patterns. Two robust distinct neuroanatomical subtypes were identified. Subtype 1 was featured with decreased motor network-related edges that might be corresponding to psychomotor retardation in depression. As a central feature of depression, psychomotor retardation was underpinned by dysfunction of brain regions including basal ganglia, motor areas and prefrontal cortex (Buyukdura, McClintock, & Croarkin, 2011). Subtype 2 was characterized by decreased edges within subcortical-cerebellum networks and exhibited significant association with reward-related function terms. Dysfunction of this network was found to be related to the anhedonia in depression (Han et al., 2020). These results suggested we uncovered two distinct neuroanatomical subtypes that might be underpinned by distinct mechanisms, providing new insights into taxonomy and facilitate potential clues to precision diagnosis and treatment of depression.

Limitations and future directions

Numbers of limitations should be considered for this study. First, results were obtained in a single dataset; future study should use another dataset to validate these results. Second, considering the remarkable difference in structural covariance aberrance, these two depression subtypes might distinctly respond to treatment. Future research studies could use longitudinal datasets to explore the potential that individualized aberrance could provide clues indicative of precision diagnosis and treatment. Third, the association between differential structural covariance edges and cognitive terms was done with the help the Neurosynth for the

https://doi.org/10.1017/S0033291722002380 Published online by Cambridge University Press

reason that we did not have corresponding scales. Fourth, factors including alcohol/cigarette and body mass index were not controlled in this study (Boden & Fergusson, 2011; Jantaratnotai, Mosikanon, Lee, & McIntyre, 2017; Mathew, Hogarth, Leventhal, Cook, & Hitsman, 2017).

Conclusion

We described individualized differential structural edges and uncovered two distinct neuroanatomical subtypes in depression for the first time. Although patients with depression demonstrated remarkable differences in the distribution of individualized altered structural covariance edges, they often shared differential edges within subcortical-cerebellum network. This result suggested that the subcortical-cerebellum network might be related to pathomechanism of depression. Two robust distinct neuroanatomical subtypes were uncovered. These two subtypes exhibited distinct patterns of differential edges while shared indistinguishable clinical and demographic features. Specially, subtype 1 often shared decreased motor network-related edges while subtype 2 often shared decreased subcortical-cerebellum network-related edges. In addition, decreased edges in subtype 2 were mainly implicated in reward/motivation-related functional terms. The identified two subtypes provide new insights into taxonomy and facilitate potential clues to precision diagnosis and treatment of depression.

Supplementary material. The supplementary material for this article can be found at https://doi.org/10.1017/S0033291722002380

Acknowledgements. This research study was supported by the Natural Science Foundation of China (81601467, 81871327, 62106229) and Medical Science and Technology Research Project of Henan province (201701011, SBGJ202102103, SBGJ202101013) and China Postdoctoral Science Foundation (2022M712890).

Conflict of interest. All authors declared no conflict of interest.

References

Ajnakina, O., Das, T., Lally, J., Di Forti, M., Pariante, C. M., Marques, T. R., & Mondelli, V. (2021). Structural covariance of cortical gyrification at illness onset in treatment resistance: A longitudinal study of first-episode psychoses. *Schizophrenia Bulletin*, *47*(6), 1729–1739. doi: 10.1093/schbul/sbab035

Alexander-Bloch, A., Giedd, J. N., & Bullmore, E. (2013). Imaging structural co-variance between human brain regions. *Nature Reviews. Neuroscience*, *14*(5), 322–336. doi: 10.1038/nrn3465

Allen, E. A., Damaraju, E., Plis, S. M., Erhardt, E. B., Eichele, T., & Calhoun, V. D. (2014). Tracking whole-brain connectivity dynamics in the resting state. *Cerebral Cortex*, *24*(3), 663–676. doi: 10.1093/cercor/bhs352

Beijers, L., Wardenaar, K. J., van Loo, H. M., & Schoevers, R. A. (2019). Data-driven biological subtypes of depression: Systematic review of biological approaches to depression subtyping. *Molecular Psychiatry*, *24*(6), 888–900. doi: 10.1038/s41380-019-0385-5

Boden, J. M., & Fergusson, D. M. (2011). Alcohol and depression. *Addiction* (*Abingdon, England*), *106*(5), 906–914. doi: 10.1111/j.1360-0443.2010.03351.x

Bondar, J., Caye, A., Chekroud, A. M., & Kieling, C. (2020). Symptom clusters in adolescent depression and differential response to treatment: A secondary analysis of the treatment for adolescents with depression study randomised trial. *The Lancet. Psychiatry*, *7*(4), 337–343. doi: 10.1016/s2215-0366(20)30060-2

Buyukdura, J. S., McClintock, S. M., & Croarkin, P. E. (2011). Psychomotor retardation in depression: Biological underpinnings, measurement, and treatment. *Progress in Neuro-Psychopharmacology & Biological Psychiatry*, *35*(2), 395–409. doi: 10.1016/j.pnpbp.2010.10.019

Chen, J., Rashid, B., Yu, Q., Liu, J., Lin, D., Du, Y., … Calhoun, V. D. (2018). Variability in resting state network and functional network connectivity associated with schizophrenia genetic risk: A pilot study. *Frontiers in Neuroscience*, *12*, 114. doi: 10.3389/fnins.2018.00114

Cheng, W., Rolls, E. T., Zhang, J., Sheng, W., Ma, L., Wan, L., … Feng, J. (2017). Functional connectivity decreases in autism in emotion, self, and face circuits identified by knowledge-based enrichment analysis. *NeuroImage*, *148*, 169–178. doi: 10.1016/j.neuroimage.2016.12.068

Cheng, Y., Xu, J., Yu, H., Nie, B., Li, N., Luo, C., … Xu, X. (2014). Delineation of early and later adult onset depression by diffusion tensor imaging. *PLoS One*, *9*(11), e112307. doi: 10.1371/journal.pone.0112307

Cole, M. W., Anticevic, A., Repovs, G., & Barch, D. (2011). Variable global dysconnectivity and individual differences in schizophrenia. *Biological Psychiatry*, *70*(1), 43–50. doi: 10.1016/j.biopsych.2011.02.010

Craddock, R. C., James, G. A., Holtzheimer, III. P. E., Hu, X. P., & Mayberg, H. S. (2012). A whole brain fMRI atlas generated via spatially constrained spectral clustering. *Human Brain Mapping*, *33*(8), 1914–1928. doi: 10.1002/hbm.21333

Das, T., Borgwardt, S., Hauke, D. J., Harrisberger, F., Lang, U. E., Riecher-Rössler, A., … Schmidt, A. (2018). Disorganized gyrification network properties during the transition to psychosis. *JAMA Psychiatry*, *75*(6), 613–622. doi: 10.1001/jamapsychiatry.2018.0391

Draganski, B., Gaser, C., Busch, V., Schuierer, G., Bogdahn, U., & May, A. (2004). Neuroplasticity: Changes in grey matter induced by training. *Nature*, *427*(6972), 311–312. doi: 10.1038/427311a

Drysdale, A. T., Grosenick, L., & Downar, J. (2017). Resting-state connectivity biomarkers define neurophysiological subtypes of depression. *Nature Medicine*, *23*(1), 28–38. doi: 10.1038/nm.4246

Evans, A. C. (2013). Networks of anatomical covariance. *NeuroImage*, *80*, 489–504. doi: 10.1016/j.neuroimage.2013.05.054

Feder, S., Sundermann, B., Wersching, H., Teuber, A., Kugel, H., Teismann, H., … Pfleiderer, B. (2017). Sample heterogeneity in unipolar depression as assessed by functional connectivity analyses is dominated by general disease effects. *Journal of Affective Disorders*, *222*, 79–87. doi: 10.1016/j.jad.2017.06.055

Finn, E. S., Shen, X., Scheinost, D., Rosenberg, M. D., Huang, J., Chun, M. M., … Constable, R. T. (2015). Functional connectome fingerprinting: Identifying individuals using patterns of brain connectivity. *Nature Neuroscience*, *18*(11), 1664–1671. doi: 10.1038/nn.4135

Goldberg, D. (2011). The heterogeneity of 'major depression'. *World Psychiatry*, *10*(3), 226–228. doi: 10.1002/j.2051-5545.2011.tb00061.x

Gong, Q., & He, Y. (2015). Depression, neuroimaging and connectomics: A selective overview. *Biological Psychiatry*, *77*(3), 223–235. doi: 10.1016/j.biopsych.2014.08.009

Gopal, S., Miller, R. L., Michael, A., Adali, T., Cetin, M., Rachakonda, S., … Calhoun, V. D. (2016). Spatial variance in resting fMRI networks of schizophrenia patients: An independent vector analysis. *Schizophrenia Bulletin*, *42*(1), 152–160. doi: 10.1093/schbul/sbv085

Han, S., Chen, Y., Zheng, R., Li, S., Jiang, Y., Wang, C., … Cheng, J. (2021a). The stage-specifically accelerated brain aging in never-treated first-episode patients with depression. *Human Brain Mapping*, *42*(11), 3656–3666. doi: 10.1002/hbm.25460

Han, S., Cui, Q., Wang, X., Chen, Y., Li, D., Li, L., … Chen, H. (2020). The anhedonia is differently modulated by structural covariance network of NAc in bipolar disorder and major depressive disorder. *Progress in Neuro-Psychopharmacology & Biological Psychiatry*, *99*, 109865. doi: 10.1016/j.pnpbp.2020.109865

Han, S., Xu, Y., Guo, H. R., Fang, K., Wei, Y., Liu, L., … Cheng, J. (2022). Resolving heterogeneity in obsessive-compulsive disorder through individualized differential structural covariance network analysis. *Cerebral Cortex*. doi: 10.1093/cercor/bhac163

Han, S., Zheng, R., Li, S., Liu, L., Wang, C., Jiang, Y., … Cheng, J. (2021b). Progressive brain structural abnormality in depression assessed with MR imaging by using causal network analysis. *Psychological Medicine*, 1–10. doi: 10.1017/s0033291721003986, (https://www.cambridge.org/core/journals/psychological-medicine/article/abs/progressive-brain-structural-abnormality-in-depressionassessed-with-mr-imaging-by-using-causal-network-analysis/2F9AFE9CCDD4D6DA9E983460780D5991).

Harald, B., & Gordon, P. (2012). Meta-review of depressive subtyping models. *Journal of Affective Disorders*, *139*(2), 126–140. doi: 10.1016/j.jad.2011.07.015

https://doi.org/10.1017/S0033291722002380 Published online by Cambridge University Press

Hasler, G. (2010). Pathophysiology of depression: Do we have any solid evidence of interest to clinicians? *World Psychiatry*, *9*(3), 155–161. doi: 10.1002/j.2051-5545.2010.tb00298.x

Hu Be Rt, L., & Arabie, P. (1985). Comparing partitions. *Journal of Classification*, *2*(1), 193–218.

Jantaratnotai, N., Mosikanon, K., Lee, Y., & McIntyre, R. S. (2017). The interface of depression and obesity. *Obesity Research & Clinical Practice*, *11*(1), 1–10. doi: 10.1016/j.orcp.2016.07.003

Kaiser, R. H., Andrews-Hanna, J. R., Wager, T. D., & Pizzagalli, D. A. (2015). Large-scale network dysfunction in major depressive disorder: A meta-analysis of resting-state functional connectivity. *JAMA Psychiatry*, *72*(6), 603–611. doi: 10.1001/jamapsychiatry.2015.0071

Kendell, R., & Jablensky, A. (2003). Distinguishing between the validity and utility of psychiatric diagnoses. *The American Journal of Psychiatry*, *160* (1), 4–12. doi: 10.1176/appi.ajp.160.1.4

Kessler, R. C., Berglund, P., Demler, O., Jin, R., Koretz, D., Merikangas, K. R., … Wang, P. S. (2003). The epidemiology of major depressive disorder: Results from the National Comorbidity Survey Replication (NCS-R). *JAMA*, *289*(23), 3095–3105. doi: 10.1001/jama.289.23.3095

Krishnan, V., & Nestler, E. J. (2008). The molecular neurobiology of depression. *Nature*, *455*(7215), 894–902. doi: 10.1038/nature07455

Lee, A., Poh, J. S., Wen, D. J., Guillaume, B., Chong, Y. S., Shek, L. P., … Qiu, A. (2019). Long-term influences of prenatal maternal depressive symptoms on the amygdala-prefrontal circuitry of the offspring from birth to early childhood. *Biological Psychiatry. Cognitive Neuroscience and Neuroimaging*, *4*(11), 940–947. doi: 10.1016/j.bpsc.2019.05.006

Lerch, J. P., Worsley, K., Shaw, W. P., Greenstein, D. K., Lenroot, R. K., Giedd, J., & Evans, A. C. (2006). Mapping anatomical correlations across cerebral cortex (MACACC) using cortical thickness from MRI. *NeuroImage*, *31*(3), 993–1003. doi: 10.1016/j.neuroimage.2006.01.042

Lima-Ojeda, J. M., Rupprecht, R., & Baghai, T. C. (2018). Neurobiology of depression: A neurodevelopmental approach. *The World Journal of Biological Psychiatry*, *19*(5), 349–359. doi: 10.1080/15622975.2017.1289240

Liu, Z., Palaniyappan, L., Wu, X., Zhang, K., Du, J., Zhao, Q., … Lin, C. P. (2021). Resolving heterogeneity in schizophrenia through a novel systems approach to brain structure: Individualized structural covariance network analysis. *Molecular Psychiatry*, *26*(12), 7719–7731. doi: 10.1038/s41380-021-01229-4

Liu, Z., Rolls, E. T., Liu, Z., Zhang, K., Yang, M., Du, J., … Feng, J. (2019). Brain annotation toolbox: Exploring the functional and genetic associations of neuroimaging results. *Bioinformatics* (*Oxford, England*), *35*(19), 3771–3778. doi: 10.1093/bioinformatics/btz128

Lv, J., Di Biase, M., Cash, R. F. H., & Cocchi, L. (2020). Individual deviations from normative models of brain structure in a large cross-sectional schizophrenia cohort. *Molecular Psychiatry*, *26*, 3512–3523. doi: 10.1038/s41380-020-00882-5

Lynch, C. J., Gunning, F. M., & Liston, C. (2020). Causes and consequences of diagnostic heterogeneity in depression: Paths to discovering novel biological depression subtypes. *Biological Psychiatry*, *88*(1), 83–94. doi: 10.1016/j.biopsych.2020.01.012

Mak, E., Colloby, S. J., Thomas, A., & O'Brien, J. T. (2016). The segregated connectome of late-life depression: A combined cortical thickness and structural covariance analysis. *Neurobiology of Aging*, *48*, 212–221. doi: 10.1016/j.neurobiolaging.2016.08.013

Mathew, A. R., Hogarth, L., Leventhal, A. M., Cook, J. W., & Hitsman, B. (2017). Cigarette smoking and depression comorbidity: Systematic review and proposed theoretical model. *Addiction* (*Abingdon, England*), *112*(3), 401–412. doi: 10.1111/add.13604

Miller, & Rupert, G. (1974). The jackknife-a review. *Biometrika*, *61*(1), 1–15.

Neufeld, N. H., & Kaczkurkin, A. N. (2020). Structural brain networks in remitted psychotic depression. *Neuropsychopharmacology: official publication of the American College of Neuropsychopharmacology*, *45*(7), 1223–1231. doi: 10.1038/s41386-020-0646-7

Okada, K., Nakao, T., Sanematsu, H., Murayama, K., Honda, S., Tomita, M., … Kanba, S. (2015). Biological heterogeneity of obsessive-compulsive disorder: A voxel-based morphometric study based on dimensional assessment. *Psychiatry and Clinical Neurosciences*, *69*(7), 411–421. doi: 10.1111/pcn.12269

Otte, C., Gold, S. M., Penninx, B. W., Pariante, C. M., Etkin, A., Fava, M., … Schatzberg, A. F. (2016). Major depressive disorder. *Nature Reviews. Disease Primers*, *2*, 16065. doi: 10.1038/nrdp.2016.65

Pezawas, L., Verchinski, B. A., Mattay, V. S., Callicott, J. H., Kolachana, B. S., Straub, R. E., … Weinberger, D. R. (2004). The brain-derived neurotrophic factor val66met polymorphism and variation in human cortical morphology. *The Journal of Neuroscience*, *24*(45), 10099–10102. doi: 10.1523/jneurosci.2680-04.2004

Price, R. B., Gates, K., Kraynak, T. E., Thase, M. E., & Siegle, G. J. (2017a). Data-driven subgroups in depression derived from directed functional connectivity paths at rest. *Neuropsychopharmacology*, *42*(13), 2623–2632. doi: 10.1038/npp.2017.97

Price, R. B., Lane, S., Gates, K., Kraynak, T. E., Horner, M. S., Thase, M. E., & Siegle, G. J. (2017b). Parsing heterogeneity in the brain connectivity of depressed and healthy adults during positive mood. *Biological Psychiatry*, *81*(4), 347–357. doi: 10.1016/j.biopsych.2016.06.023

Rashidi-Ranjbar, N., Rajji, T. K., Kumar, S., Herrmann, N., Mah, L., Flint, A. J., … Dickie, E. W. (2020). Frontal-executive and corticolimbic structural brain circuitry in older people with remitted depression, mild cognitive impairment, Alzheimer's dementia, and normal cognition. *Neuropsychopharmacology: official publication of the American College of Neuropsychopharmacology*, *45*(9), 1567–1578. doi: 10.1038/s41386-020-0715-y

Ravindran, A., Richter, M., Jain, T., Ravindran, L., Rector, N., & Farb, N. (2020). Functional connectivity in obsessive-compulsive disorder and its subtypes. *Psychological Medicine*, *50*(7), 1173–1181. doi: 10.1017/s0033291719001090

Schmaal, L., Hibar, D. P., Sämann, P. G., Hall, G. B., Baune, B. T., Jahanshad, N., … Tiemeier, H. (2017). Cortical abnormalities in adults and adolescents with major depression based on brain scans from 20 cohorts worldwide in the ENIGMA Major Depressive Disorder Working Group. *Molecular Psychiatry*, *22*(6), 900–909. doi: 10.1038/mp.2016.60

Shen, X., Tokoglu, F., Papademetris, X., & Constable, R. T. (2013). Groupwise whole-brain parcellation from resting-state fMRI data for network node identification. *NeuroImage*, *82*, 403–415. doi: 10.1016/j.neuroimage.2013.05.081

Sun, X., Liu, J., Ma, Q., Duan, J., Wang, X., Xu, Y., … Xia, M. (2021). Disrupted intersubject variability architecture in functional connectomes in schizophrenia. *Schizophrenia Bulletin*, *47*(3), 837–848. doi: 10.1093/schbul/sbaa155

Voineskos, A. N., Jacobs, G. R., & Ameis, S. H. (2020). Neuroimaging heterogeneity in psychosis: Neurobiological underpinnings and opportunities for prognostic and therapeutic innovation. *Biological Psychiatry*, *88*(1), 95–102. doi: 10.1016/j.biopsych.2019.09.004

Watanabe, K., Kakeda, S., Katsuki, A., Ueda, I., Ikenouchi, A., Yoshimura, R., & Korogi, Y. (2020). Whole-brain structural covariance network abnormality in first-episode and drug-naïve major depressive disorder. *Psychiatry Research. Neuroimaging*, *300*, 111083. doi: 10.1016/j.pscychresns.2020.111083

Wolfers, T., Doan, N. T., Kaufmann, T., Alnæs, D., Moberget, T., Agartz, I., … Marquand, A. F. (2018). Mapping the heterogeneous phenotype of schizophrenia and bipolar disorder using normative models. *JAMA Psychiatry*, *75* (11), 1146–1155. doi: 10.1001/jamapsychiatry.2018.2467

Xia, J., Fan, J., Liu, W., Du, H., Zhu, J., Yi, J., … Zhu, X. (2020). Functional connectivity within the salience network differentiates autogenous – From reactive-type obsessive-compulsive disorder. *Progress in Neuro-Psychopharmacology & Biological Psychiatry*, *98*, 109813. doi: 10.1016/j.pnpbp.2019.109813

Yarkoni, T., Poldrack, R. A., Nichols, T. E., Van Essen, D. C., & Wager, T. D. (2011). Large-scale automated synthesis of human functional neuroimaging data. *Nature Methods*, *8*(8), 665–670. doi: 10.1038/nmeth.1635

Yoo, S. Y., Roh, M. S., Choi, J. S., Kang, D. H., Ha, T. H., Lee, J. M., … Kwon, J. S. (2008). Voxel-based morphometry study of gray matter abnormalities in obsessive-compulsive disorder. *Journal of Korean Medical Science*, *23*(1), 24–30. doi: 10.3346/jkms.2008.23.1.24

Yu, M., Linn, K. A., Shinohara, R. T., Oathes, D. J., Cook, P. A., Duprat, R., & Moore, T. M. (2019). Childhood trauma history is linked to abnormal brain connectivity in major depression. *Proceedings of the National Academy of Sciences of*

https://doi.org/10.1017/S0033291722002380 Published online by Cambridge University Press

the United States of America, *116*(17), 8582–8590. doi: 10.1073/pnas.1900801116

Yun, J. Y., Jang, J. H., Kim, S. N., Jung, W. H., & Kwon, J. S. (2015). Neural correlates of response to pharmacotherapy in obsessive-compulsive disorder: Individualized cortical morphology-based structural covariance. *Progress in Neuro-Psychopharmacology & Biological Psychiatry*, *63*, 126–133. doi: 10.1016/j.pnpbp.2015.06.009

Yun, J. Y., & Kim, Y. K. (2021). Phenotype network and brain structural covariance network of major depression. *Advances in Experimental Medicine and Biology*, *1305*, 3–18. doi: 10.1007/978-981-33-6044-0_1

Zhao, Y. J., Du, M. Y., Huang, X. Q., Lui, S., Chen, Z. Q., Liu, J., … Gong, Q. Y. (2014). Brain grey matter abnormalities in medication-free patients with major depressive disorder: A meta-analysis. *Psychological Medicine*, *44*(14), 2927–2937. doi: 10.1017/s0033291714000518

https://doi.org/10.1017/S0033291722002380 Published online by Cambridge University Press